INCORPORATION OF ALLOMETRY INTO SINGLE-TREE REMOTE SENSING WITH LIDAR AND MULTIPLE AERIAL IMAGES

I. Korpela

Department of Forest Resource Management, POB 27, 00014 University of Helsinki, Finland – ilkka.korpela@helsinki.fi

KEY WORDS: Forest Inventory, Mapping, Positioning, Adjustment, Height Estimation, Crown modeling, Allometric Modeling

ABSTRACT:

A complete single-tree remote sensing (STRS) system is presented and a restricted test of performance is given. The system can be used for solving the tasks of STRS: tree positioning, height estimation species recognition, crown width estimation and estimation of the stem dimensions. The system is based on a semi-automatic approach and where automatic solutions fail, operator input is used. Knowledge in the allometry of trees is used in setting initial approximations for model-based reconstruction and in finding gross errors in observations. Multi-scale template matching is applied in simultaneous 3D treetop positioning and image-based crown width estimation. A concept of using crown modeling in combination with a relatively sparse LiDAR data is presented. The need for very high-density LiDAR is reduced, when the image-based 3D treetop positioning and species recognition are done prior to the LiDAR-based crown shape estimation as allometric constraints can be applied.

1. INTRODUCTION

1.1 Future forest inventory methods

The traditional way of measuring trees in the field is giving way to new remote sensing applications, which have different scales of observation from single trees to plots and stands. In many ways individual trees constitute a natural target of observation and single-tree remote sensing (STRS) aims at substituting the field measurements of individual trees for position, species, height, stem diameter and volume. Ideally, a STRS-based forest inventory could be carried out without field visits, as it is largely based on direct measurements of the dimensions of trees. Respectively, in area-based remote sensing methods of forests, e.g. when using characteristics of sparse LiDAR data (Naesset, 2004) or satellite images, there is a need for a representative field sample.

Different sensors or methods that encompass certain scales of observation should not be taken as exclusionary alternatives. An optimal hybrid forest inventory most likely combines different data sources and furthermore, adjusts to the information needs that vary for example between stands and forest owners. In such a vision, STRS could have a foothold provided that the single-tree estimates for position, species, height and stem dimensions are accurate enough and the costs of data acquisition and analysis remain tolerable.

1.2 Single-tree remote sensing, STRS for forestry

The idea of STRS is not novel and early articles in photogrammetric STRS date back to the 1950s (see Korpela, 2004). While the interest in the development has been extensive recently, commercial STRS systems are essentially pending on the market. There are specific difficulties and obstacles that explain this. Scene complexity is an inherent aspect of STRS. Trees vary in crown size, shape and optical properties. Crowns are often interlaced, which hinders reliable detection in images or in LiDAR surfaces and point clouds. Occlusion and shading are inherently present in images causing unpreventable omission errors. In closed boreal canopies, the trees with a relative height of above 0.5-0.7 are detectable in images. Consequently, 0-12% of the total stem volume and >0% of the stems remain unseen (Korpela 2004). The fact that small trees remain undetected is a critical shortage for many applications. However, the detectable trees constitute 90-100% of the commercial timber, which motivates for applications in timber cruising.

If we omit aspects of environmental protection or STRS in an urban environment, foresters are interested in the current and future properties of the stems and the information on available timber assortments in a given area. Improved decisions are made in silvicultural and logging operations, if this information is accurate. This pays for the data. Objectives that are set for STRS systems should reflect these information requirements. For example, the benefit of very accurate tree positions and heights is small, if the species information is lacking or it is imprecise (Korpela and Tokola, 2006).

1.3 Allometry in STRS

Because of the complexity and ill-posed nature of STRS, it seems necessary to adopt the semi-automatic approach and the use of auxiliary information to make STRS solvable. Allometry, i.e. the knowledge on the relative sizes of plant parts, is used in STRS, when the measurements of tree species, height and crown width are used for estimating the stem diameter with allometric equations (Kalliovirta and Tokola, 2005). These models are imperfect and their inaccuracy, which is in the order of 10% for stem diameter, defines an upper bound for the achievable accuracy by STRS. Allometry varies between tree species and within a stand as trees adapt to the intra- and interspecific competition and site conditions. The functioning and structure of trees are closely linked and it might be possible to improve the estimation accuracy of stem dimensions, if, for example, STRS could provide measurements of the foliage density or biomass (e.g. Ilomäki et al., 2004). Foliage mass and crown length are also linked (e.g. Kantola and Mäkelä, 2004) and it would be an option to measure the crown length by STRS.

The regularities in allometry can be used for designing filters for realistic STRS observations. The conditional distribution of crown width given tree height and species can be used for finding gross errors. In model-based STRS, allometry provides initial approximations of the model instances (e.g. Larsen and Rudemo, 1998). For example, if the position, species and tree height are known prior to the measurement of crown dimensions, it seems possible to define an approximate crown model that is adjusted to the remote sensing observations.

1.4 Objectives

A set of semi-automatic STRS methods that run on multiple images and on semi-dense, small-footprint LiDAR were developed to form an entire STRS system (Figure 1). In it, allometric regularities are used for estimating the stem dimensions from observations, and, for creating initial approximations of crown instances that are adjusted with a LiDAR point cloud in an iterative process. Following variables are measured by the system: i) Photogrammetric 3D treetop position using multi-scale template matching, ii) photogrammetric tree height using the 3D treetop position and a DTM, iii) LiDAR-based tree height, iv) species using visual image interpretation, v) image-based crown width using multi-scale template matching, vi) LiDAR-based crown width using least square adjustment of a crown model with the LiDAR point cloud and vii) stem diameter using allometric equations. The system is described in this article and a restricted performance test is given.

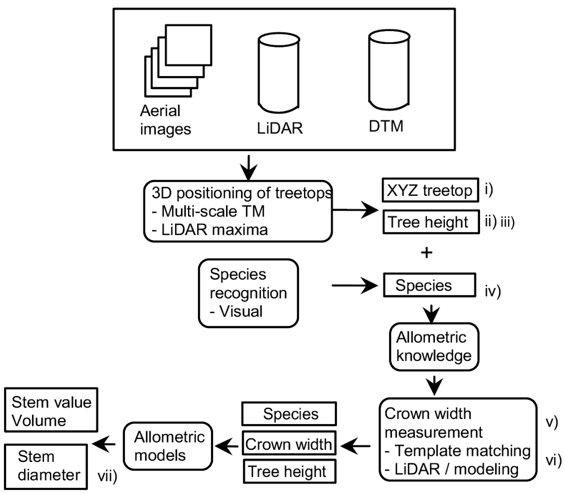

Figure 1. The data, tasks and output of the STRS-system. The measurement sequence of each tree starts with the 3D treetop positioning and is followed by height estimation, species recognition and the measurement of crown shape/width. Allometric reasoning is used in the LiDAR-based, iterative crown modelling and in the final phase, when the STRS measurements are transformed into an estimate of the stem diameter.

2. METHODS

2.1 Basic assumptions

The STRS system described in sections 2.2-2.4 assumes that multiple large-scale (> 1:15000) aerial images and a semi-dense (4-8 pulses per m^2) leaf-on LiDAR data are available and these are accurately oriented. A DTM is required for height assessment. The methods are applied in a limited area, for example in a stand or a photo-plot. Procedures described in sections 2.2-2.5 were implemented in an experimental digital photogrammetric workstation written in Visual Basic and C.

2.2 Semiautomatic photogrammetric 3D treetop positioning, height estimation and crown width estimation using multi-scale template matching

Single-scale template matching has been successfully applied in 3D treetop estimation in regular stands, where crowns have little variation (Korpela, 2004; 2007a). Here, the templates representing the crown instances in different views are copied from the real aerial images by first manually measuring the 3D treetop position of a model tree. Model trees are needed for as many species as there are in the area of interest. In the images, elliptic templates are defined that capture the upper part of the crown (Korpela, 2004 p. 36). These are copied, low-pass filtered for noise removal and scaled into N scales (scaling between 0.5 and 1.2) using bilinear re-sampling. For K images, this results in N×K templates. A treetop is pointed manually in an image that is preferred by the operator. This image observation defines a reference image-ray, which is sampled over a range in Z (Figure 2). The search range in Z is one parameter, and the search range is centered around the Z of the previously measured treetop. At each sampled 3D point along the reference image-ray, the normalized cross-correlation is computed in all images and for all templates (scales) and the mean correlation of each scale is stored. The solution of the 3D treetop position is the point with the maximum correlation. Tree height is computed next using the DTM.
The image that has the smallest oblique viewing (off-nadir) angle is selected for image-based crown width estimation using multi-scale template matching. The 3D treetop position is mapped to this image and multi-scale template matching is tried inside a small circular image window near the projection point. The template (scale) that gives the maximal cross correlation is selected and the crown width of the model tree (one of the 3 parameters that define the elliptic template of the model tree) is multiplied by the scale factor to give an image-based crown width estimate (Figure 3).

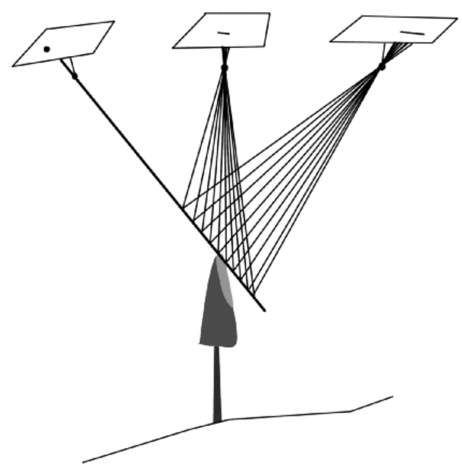

Figure 2. Illustration of the sampling of the reference image-ray over a range in Z. The treetop position in the reference image is manually observed.

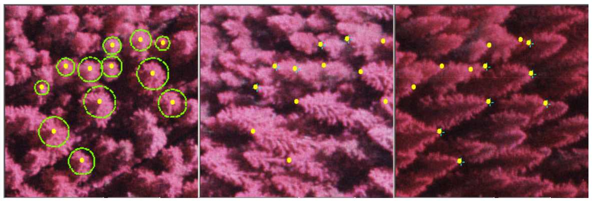

Figure 3. An example of the results of multi-scale template matching in treetop positioning and crown width estimation. A CIR-image triplet of a 28 m × 28 m area in a pine-spruce stand. Solutions of 12 treetop positions are superimposed as dots and the circles depict estimates of crown width; these are drawn in the left image that had the least off-nadir angle.

2.3 Species recognition

In preliminary tests with Vexcel Ultracam D multispectral data (28-cm R-G-B-IR-pixels) , it was found that the spectral values have considerable overlap between the three tested species: Scots pine, Norway spruce and Birch. Within a small area in the forest, and in front-lit areas of the images, the features of the IR and blue channels could be potentially used. However, the position of the tree in the image seemed to exercise a considerable effect and to cause variation in the observed spectral values. Also, young and old (vigour) trees of the same species seemed to have different spectral characteristics. The automatic approach had to be discarded for the time being and visual image interpretation was applied instead. In a large-scale CIR-image set with 60% forward and side overlaps that was available here, there are always 1-2 views, where crowns are seen back-lighted. These images are useful for separating pine and spruce. In the same study area, a 95-% overall classification accuracy was achieved by visual interpretation (Korpela 2007b). This is almost at an acceptable level in view of the accuracy requests by the foresters. The author, an experienced interpreter, carried out the visual interpretation. It was done simultaneously with the 3D treetop positioning.

2.4 Crown modelling using LiDAR points and least square adjustment

Tree crowns were approximated by a simple curve of revolution (1) that gives the crown radius $r(h_r)$ at a relative height $h_r \in [0..\pi/2]$ down from the treetop. The length of the crown is fixed to 40% of the tree height (h). The model is centred at the XYZ-position of the treetop, which is known from 3D treetop positioning. The model has three parameters and their initial values vary between species (Figure 4).

$$r(h_r) = a_1 \times h \times \sin(h_r)^{a_2} + a_3 \qquad (1)$$

Parameter a_1 sets the relationship between tree height and maximum crown radius, a_2 is a shape parameter. If a_3 deviates from zero, the top has a plateau. Using data from the National Forest Inventory of Finland (c.f. Kalliovirta and Tokola, 2005), conditional distributions of crown width given tree height and species were derived. The relationship between crown width and tree height was linear for all the three studied species: Scots pine, Norway spruce and birch. These conditional distributions were used in deriving initial or excepted ranges for the values of parameter a_1. Initial values for parameter a_2 were set such that pine and spruce had a conical crown and birch a more round crown (Figure 4). At the start of the iteration, the crown instance somewhat overestimated (by a_1) the expected crown envelope. Initial value for parameter a_3 was 0.3 m for pine and spruce and 0.5 m for birch.

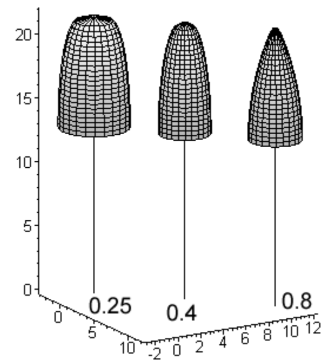

Figure 4. Illustration of three crown models for 22-m high trees (birch, pine, spruce) with varying values for the shape-parameter a_2.

The LiDAR points that were inside the initial crown instance are collected and their relative height (h_r) down from the top and the XY-distance (r) from the trunk is computed. These observations are used in solving the parameters of (1) by least square adjustment. The height of the highest LiDAR point was used as the LiDAR-based height estimate.

2.5 Allometric estimation of stem diameter

Species-specific equations by Kalliovirta and Tokola (2005) that predict the stem diameter ($d_{1.3}$) at the 1.3-m height from tree height (h) and crown width (d_{crm}) for species i were applied:

$$\sqrt{d_{1.3}} = a_i \cdot \sqrt{h} + b_i \cdot \sqrt{d_{crm}} + \varepsilon_i \qquad (2)$$

The model (2) assumes that d_{crm} is the maximal width. When the models were applied in the tests, the height estimate was always provided by the 3D treetop positioning method, and the values of d_{crm} were obtained both by LiDAR crown modeling and multi-scale template matching.

3. EXPERIMENTS

3.1 Field, image and LiDAR data

The study site is in southern Finland (61º50' N, 24º20' E). The field data consists of permanent plots, where trees have been mapped in XYZ by using 1) a tacheometer or 2) in XY by using a combined photogrammetry – field triangulation-trilateration method, in which treetops are first positioned in the images and the photo-measurable trees are identified in the field and used as control points with an observation error. Redundant observations of intertree distances and azimuths are made in the field and the positions of the undetected trees are solved using a weighted least square network adjustment (Korpela 2007b). Elevations of the plots or tree butts are known from network RTK satellite positioning and field levelling, or, the elevations were derived using a LiDAR-DTM in plots, where the trilateration-triangulation tree mapping method was applied. All trees in a plot have been observed for species and stem diameter. Heights have been observed alternatively for all trees in a plot or for a sub-set of trees. Field observations from summers 2002, 2005 or 2006 were used for reference and the effect of temporal mismatch between the different data was accounted for.

Digitized CIR-images from July 18, 2004 (time 11:25, scale 1:8000, 21-cm normal-angle optics in an RC30 camera, 12 cm GSD, 60/60% overlaps, sun elevation 45°) and digital multispectral images from August 5, 2006 (time 09:27, scale 1:10000, Vexcel UltraCam D camera, 9/28 cm GSD, 60/30% overlaps, sun elevation 30°) were used. The images were orientated in a hybrid bundle block adjustment using both direct sensor orientation observations and ground control points for the exterior orientation (Korpela 2006). For visual interpretation, the 16-bit multispectral and panchromatic Vexcel images were fused into 8-bit three-channel CIR-images having a 9-cm pixel size.

A LiDAR-DTM was estimated using TerraModeler software from a sparse, leaf-on data from August, 2004 having 0.7-2 points per m^2. Its accuracy under a canopy was estimated to be 0.27 m or better in RMSE using 8300 tacheometer points.

A semi-dense LiDAR from July 25, 2006 was available for tree crown modeling. An ALTM 3100 sensor with a pulse frequency of 100 kHz, flying height of 800 m, a scan frequency of 70 Hz, scan angle of ±14°, flying speed of 75 m/s and strip overlaps of 55% were applied in the mission. The nominal density of the data varies from 6 to 9 pulses per m^2. From 1 to 4 points per pulse with a minimum distance of 3 m between points were recorded. The LiDAR footprint was 25 cm.

3.2 Performance measures

Estimation accuracy of tree XY position, stem diameter ($d_{1.3}$), species (*Sp*) and tree height (*h*) were assessed with respect to the field measurements. Mean, SD and RMSE of the differences were used as measures of performance. Omission errors were also assessed.

3.3 Test in a dense pine-spruce stand using 6 CIR-images in the scale of 1:18000

The STRS system was tried in a dense 0.5-ha, 60-y-old pine-spruce stand, where the dominant height of the trees was 25 m (Figure 5). Trees with stem diameter of above 5 cm formed the reference data. The density was 29.9 m^2/ha in stem basal area and there were 838 stems/ha. In this stand, an intermediate felling will be done in the near future and the final felling is at the age of 80-90 years. The image, LiDAR and reference data sets had small temporal mismatches: Reference measurements were done in July 2005, the aerial photography in July 2004 and the LiDAR in July 2006. Height growth of the trees was assessed to be 0.1-0.2 m/y. Tree mapping was done with a tacheometer and the elevation was known from network RTK measurements and leveling. The plot was covered by two triplets of CIR-images in the scale of 1:8000. The STRS measurements of 347 trees took 84 minutes. Out of the 417 reference trees, 70 were missed. 19 of these were trees near a forest road, which had been broadened in 2006 prior to the LiDAR campaign. These trees could be measured from the images of 2004, but crown modeling with LiDAR failed as the trees had been felled.

The species recognition accuracy was 96.9%. An experienced operator can thus separate between pine and spruce using large-scale CIR-images. The SDs of the positioning errors for the tree stems in the X and Y were 0.23 m and 0.26 m, respectively. The absolute XY-position of the plot has not been determined so only the SDs are given.

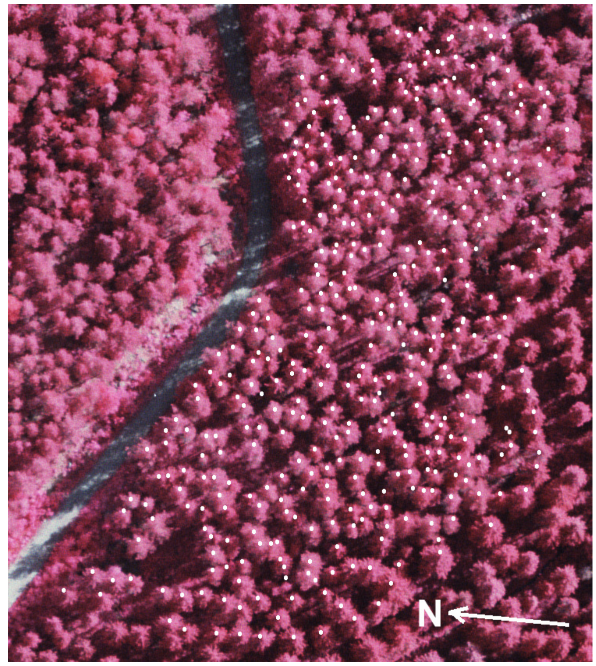

Figure 5. Field mapped treetops (height > 7 m) superimposed as white dots in a near-nadir 1:8000 CIR-image from 2004 with an off-nadir angle of 5.2°. The area in the image is 90 m × 101 m. The field plot was delimited in the field into a 0.5-ha compartment consisting of 60-y-old pines and spruces.

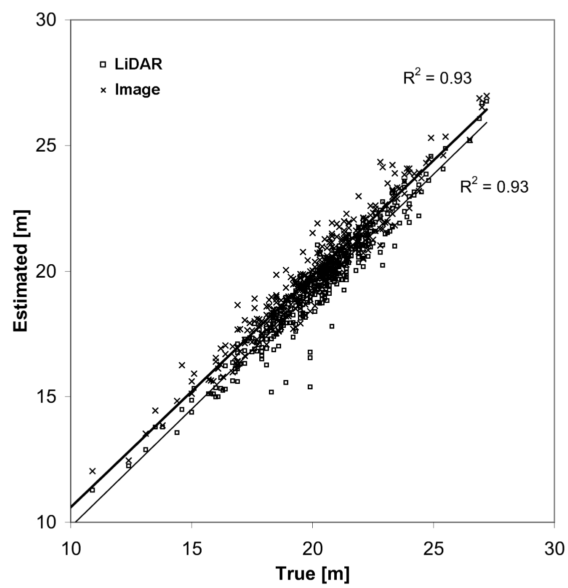

Figure 6. Distribution of true heights and estimated heights by 1) the highest LiDAR points and by 2) the image-based 3D treetop positioning using multi-scale template matching. Linear regression lines are drawn for the two data sets: thicker line is for the image-based observations.

The heights by multi-scale template matching underestimated true heights by 0.21 m and the SD of the differences was 0.63 m. The heights that were derived from the highest LiDAR points underestimated true heights by 0.83 m with an SD of

0.63 m. (Figure 6). The true underestimation of heights is actually larger, since the DTM was biased by 0.28 m and the bias compensated for the underestimation of treetop elevations. The true imprecision is also lesser than 0.63 m, because the reference data has a built-in imprecision of about 0.5 m due to field measurement errors.

Using equation (2), the visually interpreted species, the photogrammetric height and the crown width estimates by either LiDAR or multi-scale template matching were converted into stem diameter estimates. The use of LiDAR-based crown widths overestimated stem diameters by 0.86 cm with an SD of 3.2 cm (RMSE=15.9%) and the image-based crown widths underestimated stem diameters by 1.73 cm with an SD of 3.03 cm (RMSE=16.6%) (Figure 7).

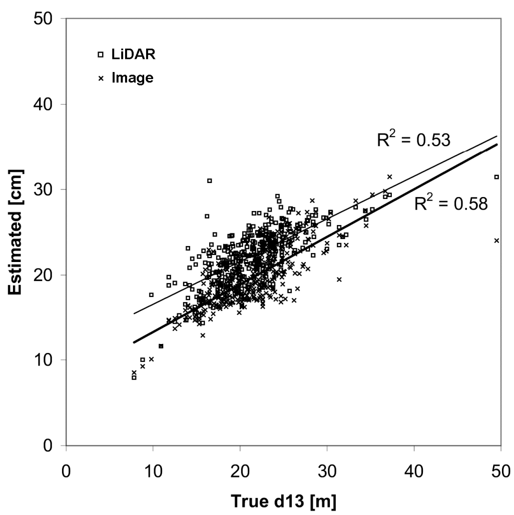

Figure 7. Distribution of the true stem diameters and the estimated values by 1) LiDAR-based crown modeling and by 2) image-based, multi-scale template matching.

3.4 Test in a 50-y-old pine stand P1

The reference data for this 50 × 50 m plot was measured in August 2002. One near-nadir CIR-image from 2004, 5 off-nadir Vexcel images from 2006 and the LiDAR from 2006 were used in the tests. It was estimated that an average height growth of about 0.6-0.8 m was missing from the reference values. Similarly, stem diameters were about 1 cm larger in 2006. The plot was visited in 2006 and undisturbed stand development was verified. Trees that could be measured constituted 94% of the total stem volume (Figure 8). Height measurements were consistent (Figure 9) and LiDAR-based heights were 0.4 m below the image-based observations. Stem diameter estimation using the crown widths by multi-scale template matching produced unsatisfactory results (Figure 10). Stem diameters were underestimated by 2.3 cm with an SD of 2.75 cm. The observed RMSE of 3.62 cm (21%) is actually larger than the SD of the true stem diameters. For LiDAR, the stem diameters were overestimated by 1.06 cm with an SD of 2.35 cm (RMSE= 14.8%). The positioning accuracy was 0.24 m for X and Y. Two (1%) errors were made in the species recognition.

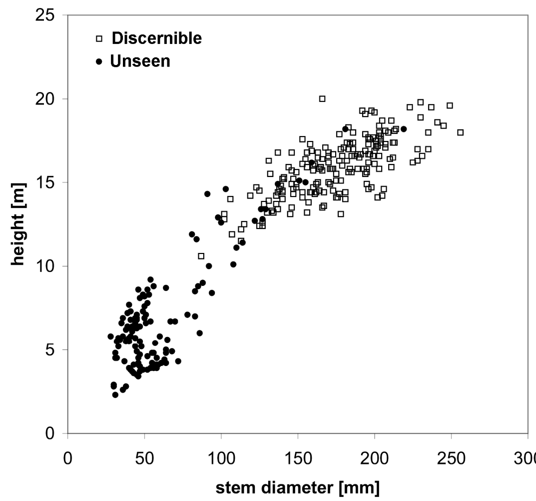

Figure 8. Pine stand P1. Stem diameter × height distribution of the detected and unseen trees. 198 of the 318 reference trees could be measured in the images and LiDAR. Even relatively high trees were missed; some of these had close neighbors and they were occluded or shaded in the images. The 50% relative height constitutes a level, where tree detection in images becomes impossible.

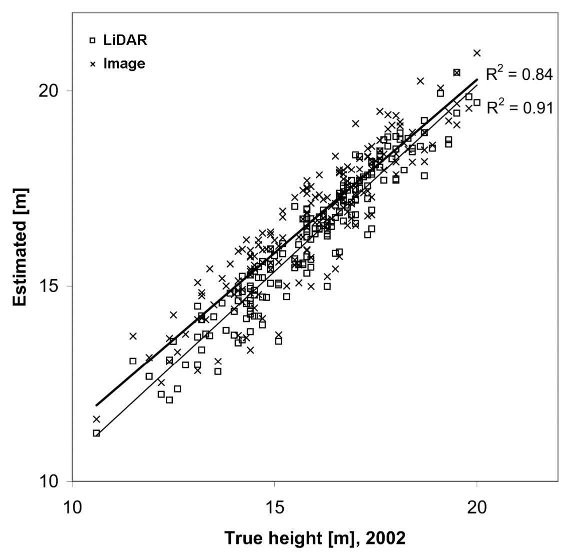

Figure 9. With the reference measurements made in 2002 and airborne data in 2006, an overestimation of heights by 0.75 m with an SD of 0.55 m and by 0.33 m with an SD of 0.73 m were observed for the image-based and LiDAR-based estimates, respectively. Annual height increment of the trees is between 0.1 - 0.3 m, which largely explains the overestimation.

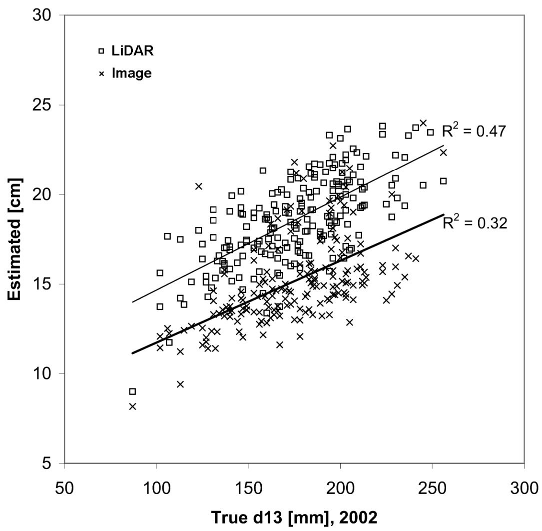

Figure 10. Distribution of the true stem diameters in 2002 and the estimated values by 1) LiDAR-based crown modeling and by 2) image-based, multi-scale template matching.

3.5 Test in a 40-y-old sparse pine-spruce stand

165 trees in area under the coverage of 3 Vexcel images were measured in a mixed, recently thinned pine-spruce stand. The species recognition accuracy was only 84.9%. No back-lighted views were available and this likely explains the poor accuracy. Height estimates had mean errors of −0.94 m and +0.03 m for the LiDAR and image-based estimation methods with SDs of 0.78 m and 0.88 m. LiDAR-derived crown widths resulted in an underestimation of stem diameters by 0.7 cm with an SD of 2.04 cm (R^2=0.68, RMSE=13%). Similarly, image-based crown width estimates resulted in an underestimation of $d_{1.3}$ by 2.1 cm with an SD of 2.5 cm (R^2=0.50, RMSE=20%). The XY positioning accuracy of the stems was 0.25 m for both X and Y. Trees in this plot were mapped in the field using the combined photogrammetry – field triangulation method.

4. DISCUSSION

The simple implementation of multi-scale template matching for image-based 3D treetop positioning worked reliably if several views of the target were available; especially if there were images from more than one flight line. However, the speed is reduced to about 200-250 trees per hour. Together with an accurate DTM, the observed height estimation accuracy varied from 0.5 to 0.8 m. The stem positions were obtained with a 0.25-m XY precision. Thus, 3D treetop positioning using multi-scale template matching offers potential and attempts to automate it can be suggested based on the findings here.

Multi-scale template matching for image-based crown width estimation in near-nadir views was successful only in one of the tested cases. In the other two tries, the use of tree heights alone would perhaps have given better results in stem diameter estimation. The implementation of the multi-scale template matching was crude, and it may well be possible to enhance the performance by developing it further. If LiDAR is not available, an image-based method for measuring the crown width is needed in an STRS system.

The results of the visual species recognition should be interpreted with caution, because they were done by one operator only, who has worked with the data for some time. An adequate accuracy of above 95% was achieved in cases, where the image set contained a back-lighted view, which are optimal for the separation between pine and spruce.

The crown modeling procedure using LiDAR points and LS-adjustment provided crown width estimates, which, when used together with height estimates for stem diameter estimation, explained from 47% to 68% of the variation in the true stem diameters. The relative RMSE of stem diameter estimation ranged from 13% to 15% and it was better than by using image-based crown width estimates (16%-21%). There is room for improvement, as the allometric models (2) have a model error of 10%; the upper bound in achievable accuracy. Again, the implementation here was simple and there are many ways of improving it. In dense areas of the forest branches overlap and the points that are used for crown surface modeling have echoed from the neighboring trees as well. If the 3D treetop positioning of all trees is done first, it might be possible to construct geometric filters and only those directions or sectors, which are free from neighboring trees, would be used selecting the LiDAR points for crown modeling. Also, it is necessary to make the height of the crown a parameter, since crown length would improve the estimation accuracy of stem dimensions.

5. REFERENCES

Ilomäki, S., Nikinmaa, E. and Mäkelä, A. 2003. Crown rise due to competition drives biomass allocation in silver birch. *Canadian Journal of Forest Research* 33 (12), pp. 2395-2404.

Kantola, A, and Mäkelä,A. 2004. Crown development in Norway spruce [Picea abies (L.) Karst.]. *Trees - Structure and Function* 18 (4), pp. 408-421

Kalliovirta, J. & Tokola, T. 2005. Functions for estimating stem diameter and tree age using tree height, crown width and existing stand database information. *Silva Fennica* 39(2), pp: 227-248.

Korpela, I. 2004. Individual tree measurements by means of digital aerial photogrammetry. *Silva Fennica Monographs*, 3, pp. 1-93.

Korpela I. 2006. Geometrically accurate time series of archived aerial images and airborne lidar data in a forest environment. *Silva Fennica,* 40(1), pp. 109-126.

Korpela, I. 2007a. 3D treetop positioning by multiple image matching of aerial images in a 3D search volume bounded by lidar surface models. *Photogrammetrie, Fernerkundung, Geoinformation* 1/2007, pp. 35-44.

Korpela, I. 2007b. Mapping forest plots: An efficient method combining photogrammetry and field triangulation. To appear in *Silva Fennica*.

Korpela, I. and Tokola, T. 2006. Potential of aerial image-based monoscopic and multiview single-tree forest inventory - a simulation approach. *Forest Science*, 52(3), pp. 136-147

Larsen, M. and Rudemo, M. 1998. Optimizing templates for finding trees in aerial photographs. *Pattern Recognition Letters* 19(12): 1153–1162.

Naesset, E. 2004. Practical large-scale forest stand inventory using a small-footprint airborne scanning laser. *Scandinavian Journal of Forest Research* 19(2), pp. 164-179.